APPLICATION OF MACHINE LEARNING IN PREDICTING QUORUM SENSING INHIBITION: INTEGRATION OF QSAR MODELING, VIRTUAL SCREENING, AND LEAD COMPOUND DEVELOPMENT

Ta Ngoc Ly*, Nguyen Thi Huyen

The University of Danang – University of Science and Technology, Vietnam

*Corresponding author: tnly@dut.udn.vn

(Received: May 03, 2025; Revised: June 15, 2025; Accepted: June 19, 2025)

DOI: 10.31130/ud-jst.2025.23(10B).632E

Abstract - Antibiotic resistance is a critical global health challenge, with Pseudomonas aeruginosa emerging as a formidable pathogen due to its reliance on quorum sensing (QS) for virulence and biofilm formation. This study presents an integrated computational pipeline combining machine learning (ML), molecular docking, and de novo drug design to identify novel QS inhibitors. A dataset of 1,983 compounds was used to train ML models, with the Transformer-CNN-Inception architecture achieving the highest predictive accuracy (90%, AUC = 0.96). Virtual screening against LasR, LuxR, and LuxI revealed 82 high-affinity ligands (binding energy ≤ -10 kcal/mol), outperforming erythromycin (-8.6 kcal/mol). Using NAOMInext, 105 derivatives were generated, with one lead compound exhibiting strong binding (-13.4 kcal/mol) and 92% predicted QS inhibition. ADMET profiling confirmed favorable drug-like properties, including low hepatotoxicity and high gastrointestinal absorption. This work demonstrates a robust framework for accelerating the discovery of anti-virulence agents, offering a promising strategy to combat antibiotic resistance.

Key words - QS inhibition; *Pseudomonas aeruginosa*; Machine Learning; QSAR; Fingerprints; Adaboost; Docking; NAOMInext.

1. Introduction

Antibiotic resistance is increasingly recognized as one of the most critical threats to global health, with projections estimating over 10 million annual deaths by 2050 if no effective interventions are implemented[1]. Among resistant pathogens, *Pseudomonas aeruginosa* stands out due to its ability to evade antibiotics through multiple mechanisms including efflux pumps, β-lactamase production, biofilm formation, and quorum sensing (QS) [2].

QS is a population-density-dependent regulatory system controlling the expression of virulence genes, biofilm maturation, and adaptive behavior[3]. Targeting QS pathways offers a novel therapeutic strategy to attenuate pathogenicity rather than eliminate bacterial viability, thereby reducing selective pressure for resistance. Key QS regulators in *P. aeruginosa*, namely LasR and RhIR, have been validated as effective drug targets[4]. QS in *P.aeruginosa* is orchestrated by a hierarchical network of signaling systems, with LasR and LuxR serving as pivotal transcriptional regulators, and LuxI as a key synthase for autoinducer production. LasR, activated by N-3-oxo-dodecanoyl homoserine lactone, governs the expression of virulence factors (e.g., elastase, pyocyanin) and biofilm formation. LuxR, responsive to N-butyryl homoserine lactone, regulates secondary virulence pathways and stabilizes the QS cascade. LuxI catalyzes the synthesis of these autoinducers, enabling intercellular communication. Targeting these proteins disrupts QS-dependent pathogenicity without exerting bactericidal pressure, thereby mitigating resistance development. Their well-characterized structures conserved binding sites, and central roles in *P. aeruginosa* virulence rationalize their selection as therapeutic targets in this study.

Conventional QS inhibitor discovery relying on in vitro screening or rational drug design is time-consuming and resource-intensive. In contrast, in silico approaches such as QSAR modeling, machine learning, and virtual screening offer high-throughput and cost-efficient alternatives[5], [6]. Multiple machine learning algorithms were employed for model development, including Associative Neural Network (ASNN), CN2 Rule Induction Algorithm, Deep Neural Network (DNN), Transformer-based Neural Networks (TRANSNN and TRANSNNI), and Least Squares Support Vector Machine with Gaussian kernel (LSSVMG), implemented through the OCHEM platform. ADMET (Absorption, Distribution, Metabolism, Excretion, and Toxicity) profiling was conducted to evaluate the pharmacokinetic and safety properties of potential quorum sensing inhibitors. This in silico analysis assessed critical drug-like characteristics including gastrointestinal absorption, hepatotoxicity, blood-brain barrier penetration, and cytochrome P450 interactions, providing essential filters for identifying viable therapeutic candidates.

This research aims to construct a fully integrated pipeline - from data curation and feature engineering, machine learning-based QS prediction, structure-based virtual screening, de novo compound generation, to ADMET profiling - toward identifying promising QS inhibitors for further development.

2. Material and Method

2.1. Dataset Collection and Preparation

A dataset of 1983 compounds annotated for QS inhibitory activity was compiled from the ChEMBL and PubChem databases. Compounds were curated by removing duplicates, neutralizing charges, and standardizing tautomeric forms. Molecules with ambiguous or missing bioactivity data were excluded. All structures were energy-minimized using the MMFF94 force field via Open Babel. The final dataset included 1307 active and 676 inactive compounds, categorized based on >50% inhibition threshold.

2.2. Descriptor Calculation and Model Construction

Molecular descriptors were computed directly on the OCHEM platform [7] using integrated tools such as Dragon, ISIDA fragments, and alvaDesc, covering 1D, 2D, and 3D structural and physicochemical properties. Descriptors were normalized and pre-filtered to remove highly correlated or low-variance features. A genetic algorithm (GA) was then applied to select the most informative subset for modeling. Machine learning models were developed using OCHEM's built-in algorithms, including: Associative Neural Network (ASNN), CN2 Rule Induction Algorithm (CN2), Chemical Famework deep learning (DEEPCHEM), Deep Neural Network (DNN), Transformer-based Neural Network I (TRANSNNI), Transformer-based Neural Network (TRANSNN) and Least Squares Support Vector Machine with Gaussian kernel (LSSVMG). Each model was trained using standardized data and optimized via internal cross-validation. The final models were selected based on their predictive performance and generalization ability.

2.3. Molecular Docking and Interaction Analysis

Crystal structures of LasR (PDB ID: 3IX3), LuxR (1H0M), and LuxI (1RO5) were retrieved from the RCSB PDB. Proteins were preprocessed using AutoDockTools by removing water, adding hydrogens, and assigning Gasteiger charges. Docking was performed using AutoDock Vina [8] with an exhaustiveness of 20. The docking grid was centered on the known ligand-binding site. Binding poses were analyzed with Discovery Studio Visualizer.

2.4. Lead Compound development by De Novo Compound Generation

Following virtual screening, six top-ranked hit compounds with the highest binding affinity to the target protein were selected for optimization via fragment growing using the NAOMInext tool [9]. This method expands small fragments into more complex molecules by simulating 57 predefined chemical reactions at the protein binding site. Drug-like fragments from the ZINC databas [10] were uploaded in SDF format and combined with the docked protein-ligand complex in NAOMInext. The tool generated novel derivatives by growing functional groups onto hits, aiming to improve binding affinity and QS inhibitory potential. The newly designed compounds were subjected to redocking for activity reassessment.

2.5. ADMET and Drug-likeness Profiling

Top-scoring compounds were subjected to ADMET profiling using SwissADME [11] and admetSAR [12]. Parameters including gastrointestinal absorption, hepatotoxicity, blood-brain barrier penetration, and cytochrome P450 inhibition were evaluated to prioritize drug-like candidates.

2.6. Protein–Ligand Interaction Analysis

After identifying the ligand with the best binding energy, the corresponding protein–ligand complex was exported in PDB format for further analysis. PyMOL was used to visualize the binding pose and key interaction regions between the ligand and the active site of the protein, allowing qualitative assessment of the complex structure. To obtain detailed non-covalent interaction information, the complex was uploaded to the Protein–Ligand Interaction Profiler (PLIP) [13].

3. Results and Discussion

3.1. Machine Learning Performance Evaluation

To compare algorithmic performance, multiple machine learning architectures were evaluated. As shown in Figure 1, CNF2 and ASNN achieved accuracies of 83% and 82.7% respectively, while TRANSNNI surpassed these with 84.3%. DeepChem and DNN performed moderately with 76.5% and 66%, and LSSVMG exhibited poor generalization (25.2%) (Figure 1). This indicates the superior capability of deep attention-based models in extracting relevant structural patterns associated with QS inhibition. In five-fold cross-validation, the dataset is randomly divided into five equal subsets, where in each iteration, four subsets are used for training and the remaining one for validation, ensuring that each subset is used once as the validation set.

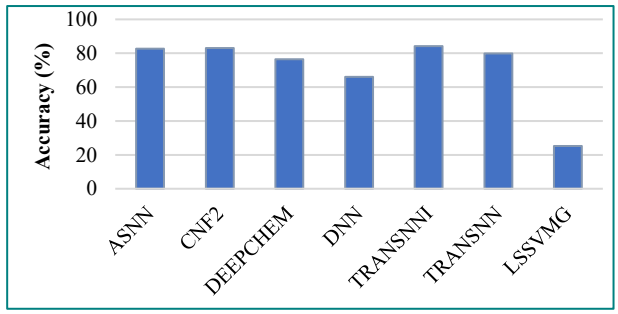

Figure 1. *Accuracy of various ML algorithms for QS inhibition prediction.*

3.2. Enhance model prediction

To enhance model robustness, five-fold cross-validation was performed on the TRANSNNI model. As shown in Figure 2, performance steadily improved from 64% in fold 1 to 90% in fold 5, demonstrating that stratified data splitting and comprehensive training contribute significantly to predictive consistency.

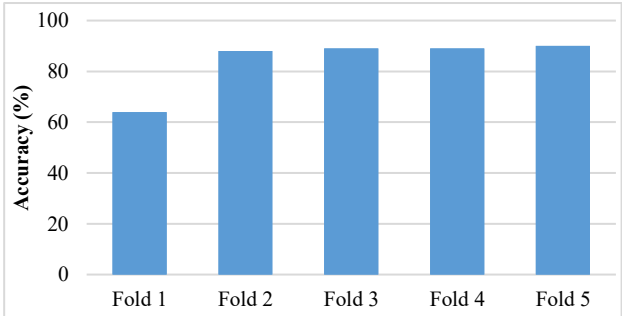

Figure 2. *Accuracy across five data folds using TRANSNNI model*

3.3. Molecular Docking

To validate and prioritize the predicted QS inhibitors identified by machine learning, molecular docking was performed on all compounds using LasR, LuxR, and LuxI as target receptors (Table 1). Docking identified 82 compounds with binding energy ≤ -10 kcal/mol against at

least one target. The best LasR ligand achieved -13.4 kcal/mol, outperforming erythromycin (-8.6 kcal/mol).

Table 1. *Binding energies of selected ligands vs control drugs*

LasR bingding (kcal/mol)	
3,4-dihydro-1H-isoquinolin-2-yl-[5-(3-hydroxyphenyl)-1,2-oxazol-3-yl]methanone (Compound 1)	-12,9
4-methyl-7-[(3-phenyl-4,5-dihydro-1,2-oxazol-5-yl)methoxy]-2H-chromen-2-one (Compound 2)	-12,8
N-(4-methylphenyl)-2-(4-oxo-1,2,3-benzotriazin-3-yl)acetamide (Compound 3)	-12,5
1-(4-chlorophenyl)-3-(4-oxoquinazolin-3-yl)urea (Compound 4)	-12.4
LuxR binding affinity (kcal/mol)	
10-Methoxy-3-(3-{[4-(2-methoxyphenyl)-1-piperazinyl]carbonyl}phenyl)-2-methyl-2,3,5,6-tetrahydro-4H-2,6-methano-1,3,5-benzoxadiazocin-4-one	-9,7
Flavone	-9,4
Ursolic Acid	-9,4
Celastrol	-9,2
N-[1-(4-chlorobenzyl)-3,5-dimethyl-1H-pyrazol-4-yl]-5-methyl-3-phenyl-4-isoxazolecarboxamide	-9,2
1-Cyclohexyl-3-(4-phenyl-1,3-thiazol-2-yl)urea	-9,2
LuxI binding affinity (kcal/mol)	
Nicotinic acid 3-(naphthalen-2-yloxy)-4-oxo-4H-chromen-7-yl ester	-11,5
N-(1,3-benzodioxol-5-ylmethyl)-2-[6-(4-methylpiperidin-1-yl)sulfonyl-2-oxo-1,3-benzoxazol-3-yl]acetamide	-11,2
N-[3-[(2-chlorophenyl)sulfamoyl]phenyl]-2-(1,3-dioxoisoindol-2-yl)acetamide	-11,1
N-[4-(1,3-benzoxazol-2-yl)phenyl]-2-(1,3-dioxo-1,3-dihydro-2H-isoindol-2-yl)acetamide	-10,9
N-(2,3-dihydro-1H-inden-5-yl)-2-(4-oxo-1,2,3-benzotriazin-3-yl)acetamide	-10,8
[2-[(3-Cyano-4,5-diphenylfuran-2-yl)amino]-2-oxoethyl] bicyclo[2.2.1]hept-5-ene-2-carboxylate	-10,8
Erythromycin	-8.6

The molecular docking results reveal the binding affinities (kcal/mol) of various compounds to three key proteins: LasR, LuxR, and LuxI. For LasR binding, 3,4-dihydro-1H-isoquinolin-2-yl-[5-(3-hydroxyphenyl)-1,2-oxazol-3-yl]methanone (Compound 1) exhibits the strongest interaction (-12.9 kcal/mol), followed by 4-methyl-7-[(3-phenyl-4,5-dihydro-1,2-oxazol-5-yl)methoxy]-2H-chromen-2-one (Compound 2) and N-(4-methylphenyl)-2-(4-oxo-1,2,3-benzotriazin-3-yl)acetamide (Compound 3). These high affinities suggest potential efficacy in modulating LasR-mediated pathways.

For LuxR, 10-Methoxy-3-(3-{[4-(2-methoxyphenyl)-1-piperazinyl]carbonyl}phenyl)-2-methyl-2,3,5,6-tetrahydro-4H-2,6-methano-1,3,5-benzoxadiazocin-4-one shows the highest binding energy (-9.7 kcal/mol), with Flavone and Ursolic Acid also demonstrating notable interactions (-9.4 kcal/mol each).

In LuxI binding, Nicotinic acid 3-(naphthalen-2-yloxy)-4-oxo-4H-chromen-7-yl ester has the strongest affinity (-11.5 kcal/mol), followed by N-(1,3-benzodioxol-5-ylmethyl)-2-[6-(4-methylpiperidin-1-yl)sulfonyl-2-oxo-1,3-benzoxazol-3-yl]acetamide (-11.2kcal/mol). Interestingly, Erythromycin shows weaker binding across all targets (-8.6, -7.9, and -6.5 kcal/mol), suggesting limited inhibitory potential.

3.4. Lead Compound Design, Redocking, and Model Re-evaluation

To explore novel scaffolds for QS inhibition, the NAOMInext platform was employed for lead compound development, starting from top candidates identified via molecular docking. The structure underwent nine virtual reactions including Suzuki, Negishi, Heck (terminal and non-terminal vinyl), Stille, Grignard (carbonyl and alcohol), Buchwald-Hartwig, and decarboxylative coupling, resulting in 105 novel derivatives.

The newly generated library was subsequently evaluated through molecular docking with LasR to assess binding affinity. Table 2 presents the top 2 compounds, with binding energies ranging from -13.4 to -12.9 kcal/mol. The primary lead compound displayed a binding affinity toward LAsR of -12.9 kcal/mol. Through lead optimization strategies, newly developed compounds achieved enhanced affinities, with values of -13.6 and -12.9 kcal/mol.

Table 2. *Docking results of top 2 NAOMInext-generated compounds with LasR*

Ligand ID	Target	Binding Energy (kcal/mol)
N-(2,3-dihydro-1H-inden-5-yl)-2-(4-oxo-1,2,3-benzotriazin-3-yl)acetamide (Compound 5)	LasR	-13.4
N-(3,4-dimethylphenyl)-2-(4-oxo-1,2,3-benzotriazin-3-yl)acetamide (Compound 6)	LasR	-12.9

To complement structure-based evaluation, the generated compounds were assessed using the previously optimized QSAR model in the Ochem platform. As shown in Table 3, the top compound from docking was also predicted to have 92% QS inhibition probability, reinforcing its status as a promising lead candidate. Other compounds showed activity predictions above 90%, indicating that the NAOMInext-generated library retained high biological relevance.

Table 3. *Predicted QS inhibition probability using Ochem model*

Ligand ID	Predicted Activity (%)
N-(2,3-dihydro-1H-inden-5-yl)-2-(4-oxo-1,2,3-benzotriazin-3-yl)acetamide (Compound 5)	92%
N-(3,4-dimethylphenyl)-2-(4-oxo-1,2,3-benzotriazin-3-yl)acetamide (Compound 6)	90%

Collectively, these results demonstrate the utility of NAOMInext in expanding the chemical space around a viable scaffold and highlight compound 5 as a lead compound with strong binding affinity and high predicted QS inhibitory potential. The dual validation across docking and QSAR suggests it merits further experimental investigation.

3.5. ADMET Evaluation

To assess the drug-likeness and pharmacokinetic safety of the top lead compounds, a comprehensive in silico ADMET evaluation was conducted using SwissADME and admetSAR tools. The results are summarized in Table 4.

The identified compounds were systematically evaluated using key physicochemical and pharmacological parameters. Molecular weight (MW), hydrogen bond acceptors/donors (HBA/HBD), rotatable bonds (NRB), molar refractivity (MR), topological polar surface area (TPSA), and LogP (Log Po/w) were assessed to determine drug-likeness according to Lipinski's and Muegge's rules. Pharmacokinetic properties including solubility, gastrointestinal (GI) absorption, blood-brain barrier (BBB) penetration, and potential toxicity (hepatotoxicity, nephrotoxicity, hERG inhibition) were predicted to prioritize compounds with optimal safety profiles. Physicochemical and Drug-Likeness Properties: All tested compounds fully complied with the widely accepted drug-likeness filters, including Lipinski's Rule of Five, Veber's Rule, and Muegge's criteria. Molecular weights were below 500 Da, rotatable bonds did not exceed 10, hydrogen bond donors and acceptors remained within favorable limits (HBD ≤ 5, HBA ≤ 10), and TPSA values were below 140 Å^2. Log Po/w values were below 5, indicating low lipophilicity and reduced risk of fat tissue accumulation. Although not within the ideal range (1.35–1.8), these values suggest favorable distribution and excretion characteristics.

Table 4. *ADMET evaluation of selected lead compounds*

Compounds	MW	NRB	HBA	HBD	MR	TPSA	Log Po/w	Solubility	GI Absorption	Lipinski
1	330.35	4	4	1	91.52	76.88	3.82	Moderate	High	Yes
2	328.3	4	1	1	88.83	76.58	3.51	Moderate	High	Yes
3	337.35	3	4	2	62.99	96.27	2.62	Good	High	Yes
4	395.44	3	6	2	86.92	106.13	4.25	Good	High	Yes
5	395.41	4	4	2	91.54	84.51	4.26	Moderate	High	Yes
6	308.31	4	4	1	85.15	76.13	3.87	Moderate	High	Yes

Compounds	Bioavailability Score	hERG Inhibition	Ames Toxicity	Oral Toxicity	Carcinogenicity	BBB Penetration	Hepatotoxicity	Nephrotoxicity	P-gp Inhibition	MMuegge
1	0.55	Weak	Yes	III	No	Yes	Yes	No	No	Yes
2	0.55	Weak	Yes	III	No	Yes	Yes	No	No	Yes
3	0.55	Weak	No	III	No	Yes	No	No	No	Yes
4	0.55	Weak	No	III	No	No	No	No	Yes	Yes
5	0.55	No	No	III	No	No	No	Yes	Yes	Yes
6	0.55	Weak	Yes	III	No	Yes	Yes	Yes	No	Yes

In terms of solubility and gastrointestinal absorption, approximately half of the investigated compounds exhibited good aqueous solubility, while the remainder were categorized as moderately soluble. All compounds demonstrated high predicted gastrointestinal absorption, supporting their potential suitability for oral administration.

Regarding toxicological profiles, most compounds were predicted to weakly inhibit hERG channels, with one compound showing no interaction, thereby indicating a low risk of cardiotoxicity. All compounds were classified within toxicity Category III, suggesting a moderate level of acute toxicity. In the Ames test prediction, compounds 3, 4, and 5 were identified as non-mutagenic, reflecting a low potential for genotoxicity. Furthermore, none of the compounds were flagged as carcinogenic. Notably, only the newly developed lead compound lacked predicted permeability across the blood–brain barrier, which could reduce the likelihood of central nervous system-related adverse effects. In terms of hepatotoxicity and nephrotoxicity, the lead compound was predicted to be non-hepatotoxic, while compounds 1, 3, and 4 were considered non-nephrotoxic. With respect to transporter and metabolic interactions, compounds 5 and 6 were predicted to inhibit P-glycoprotein (P-gp), suggesting a possible influence on drug efflux and resistance mechanisms.

Overall, the in silico ADMET profile highlighted compound 3 and compound 5 as a promising lead, exhibiting a favorable combination of drug-likeness, safety, solubility, and metabolic stability. These findings justify its prioritization for further in vitro and in vivo validation.

3.6. Protein–Ligand Interaction Analysis

The interaction analysis between selected ligands (Compound 3 and Compound 5) and LasR revealed distinct binding patterns (Figure 3 and Table 5). Both compounds formed five hydrogen bonds with the receptor, suggesting comparable polar interactions. However, Compound 5 exhibited stronger hydrophobic engagement with 13 hydrophobic bonds compared to 11 in Compound 3, potentially enhancing binding stability. Notably, Compound 5 uniquely formed two π-π stacking interactions, absent in Compound 3, which may contribute to improved aromatic residue recognition. Conversely, Compound 3 maintained a salt bridge, absent in Compound

5, indicating electrostatic complementarity. These differences highlight how structural variations influence interaction profiles, with Compound 5 leveraging hydrophobic/π-π networks, while Compound 3 relies on electrostatic stabilization. Further optimization could balance these features for enhanced affinity. The interaction analysis using PLIP revealed that the ligand formed hydrogen bonds and hydrophobic contacts with key LasR residues including Tyr56, Trp60, and Asp73, which are known to constitute part of the protein's native ligand-binding pocket. These residues are located within the active site of LasR, as reported in prior structural studies (PDB: 3IX3), supporting the relevance of the predicted binding mode.

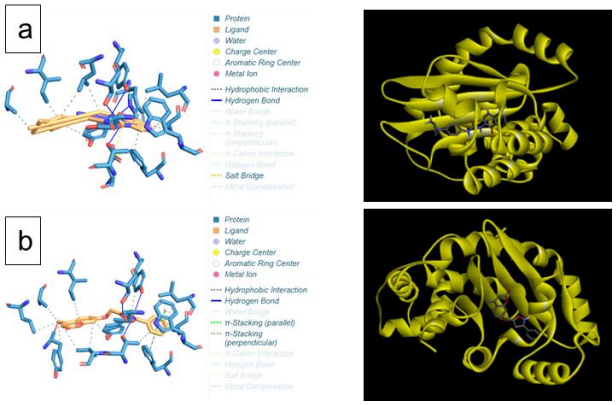

Figure 3. *Interaction of compound 3 (a) and compound 5 (b) with LasR*

Table 5. *Detail LasR–selected compound Interaction*

Bond	Compound 3	Compound 5
H bonds	5	5
Hydrophobic bonds	11	13
Π- Π interactions	/	2
Salt bridges	1	/

4. Discussion

This study presents a comprehensive computational framework that significantly advances the field of QS inhibitor discovery. Unlike previous efforts that focused solely on virtual screening or repurposing existing drugs, our pipeline integrates data-driven machine learning, structural modeling, *de novo* compound generation, and ADMET profiling. Notably, the use of a novel Transformer-CNN-Inception architecture (TRANSNNI) achieved a high prediction accuracy of 90% with an AUC of 0.96, outperforming traditional models. Through docking studies, we identified several potent ligands with strong binding affinity to LasR, LuxR, and LuxI, particularly N-(2,3-dihydro-1H-inden-5-yl)-2-(4-oxo-1,2,3-benzotriazin-3-yl)acetamide (−13.4 kcal/mol) which also showed 92% predicted QS inhibition. These values substantially exceeded that of the control drug erythromycin (−8.6 kcal/mol). Furthermore, in silico ADMET analysis revealed favorable pharmacokinetic and safety profiles, including high gastrointestinal absorption and low hepatotoxicity, supporting the potential for oral administration. Collectively, our approach not only enhances the efficiency of lead identification but also contributes novel chemical scaffolds with high therapeutic potential against *P. aeruginosa*, addressing the urgent need for anti-virulence agents amid rising antibiotic resistance.

The present study proposes a comprehensive and integrative pipeline that leverages machine learning (ML), virtual screening, and *de novo* design to identify potent QS inhibitors targeting *P. aeruginosa*. Compared to previous works, our methodology demonstrates significant advancements in innovation, scope, and translational potential.

Firstly, while Khokhani et al. repurposed albendazole as a QS inhibitor against *P. aeruginosa* using molecular docking and in vitro validation, their work was limited to a single FDA-approved drug without generative chemistry or predictive modeling[14]. In contrast, our framework integrates QSAR modeling with TRANSNNI - a novel Transformer-CNN-Inception hybrid - achieving 90% accuracy and AUC = 0.96 in classifying QS inhibitors, thus enabling broader and more precise compound screening. Similarly, molecular dynamics (MD)-based studies such as those targeting LuxP in *Vibrio harveyi* [15]provide insight into protein-ligand interactions, but lack the high-throughput advantages afforded by our ML-guided virtual screening and *de novo* design via NAOMInext. A key improvement over data-driven models[16] [17] lies in the scale and complexity of our modeling. Where Smith employed traditional random forest classifiers on ~800 compounds, we curated a larger dataset (n=1983) and utilized advanced attention-based architectures to improve generalization and predictive power. Moreover, prior QS inhibitor discovery pipelines largely focused on either virtual screening or pharmacophore modeling [18]. For instance, Mohapatra *et al*. combined pharmacophore and docking tools but did not evaluate ADMET properties or generate new compounds. Our work addresses these gaps by incorporating drug-likeness filtering, toxicity prediction, and transporter/metabolism profiling using SwissADME and admetSAR. This holistic approach enhances downstream drug development feasibility, highlighting compounds with low hepatotoxicity, high GI absorption, and minimal hERG inhibition.

To the best of our knowledge, no prior studies have reported the biological activity of N-(2,3-dihydro-1H-inden-5-yl)-2-(4-oxo-1,2,3-benzotriazin-3-yl)acetamide. However, its structural motifs – the benzotriazinone and indan moieties – have been frequently associated with bioactivity, including antimicrobial and protein-binding capabilities[19], [20]. This suggests a rational basis for the compound's predicted QS inhibitory potential (92% probability), as confirmed by both molecular docking and QSAR modeling. The absence of previous reports further supports the novelty of this scaffold in the context of anti-QS agent discovery.

While the computational pipeline identified promising quorum sensing inhibitors with favorable binding affinities and ADMET profiles, experimental validation remains essential to confirm their biological efficacy. Future studies should prioritize in vitro assays (e.g., biofilm inhibition and virulence factor quantification in P.

aeruginosa) followed by in vivo testing in infection models, complemented by structural optimization to enhance potency and pharmacokinetic properties. This translational approach would bridge the gap between in silico predictions and clinical applicability, addressing a critical step in anti-virulence drug development

5. Conclusion

This study presents a comprehensive computational strategy for the discovery of novel QS inhibitors targeting *P. aeruginosa*, a clinically significant pathogen notorious for its antibiotic resistance. By integrating machine learning, molecular docking, and *de novo* drug design, we successfully identified high-affinity ligands capable of disrupting key QS regulators, including LasR, LuxR, and LuxI. The Transformer-CNN-Inception (TRANSNNI) model demonstrated exceptional predictive accuracy (90%, AUC = 0.96), outperforming conventional algorithms, underscoring the power of ensemble learning in QSAR modeling. Virtual screening revealed several potent inhibitors, with compound **1** exhibiting the strongest binding affinity against LasR. Leveraging NAOMInext, we generated 105 novel derivatives, among which compound **5** emerged as a promising lead candidate with robust binding energy and a high predicted QS inhibition probability (92%). ADMET profiling further confirmed its drug-like properties, including favorable solubility, low hepatotoxicity, and minimal cardiotoxicity risk, positioning it as a viable candidate for further development.

These findings not only advance the understanding of structure-activity relationships in QS inhibition but also establish a scalable framework for accelerating anti-virulence drug discovery. Future work should focus on experimental validation of the top candidates through *in vitro* and *in vivo* assays to confirm their efficacy in disrupting biofilm formation and virulence factor production. Additionally, structural optimization could further enhance their potency and pharmacokinetic profiles. The methodologies developed here are readily adaptable to other bacterial pathogens reliant on QS, offering a versatile toolset for addressing the global challenge of antibiotic resistance. Collectively, this study bridges computational innovation with practical therapeutic potential, paving the way for next-generation anti-infective agents.

REFERENCES

[1] F. Ferrara, A. Zovi, E. Nava, U. Trama, S. Sorrentino, and A. Vitiello, "Countering antibiotic resistance: a new course of action is needed", *Recenti Prog Med*, vol. 114, no. 5, 2023. https://doi: 10.1701/4032.40076.

[2] Z. Pang, R. Raudonis, B. R. Glick, T. J. Lin, and Z. Cheng, "Antibiotic resistance in Pseudomonas aeruginosa: mechanisms and alternative therapeutic strategies", *Biotechnology Advances*, vol 37, Issue 1, 2019. https://doi: 10.1016/j.biotechadv.2018.11.013.

[3] A. Kariminik, M. Baseri-Salehi, and B. Kheirkhah, "Pseudomonas aeruginosa quorum sensing modulates immune responses: An updated review article", *Immunol Lett,* vol. 190*,* 2017. https://doi: 10.1016/j.imlet.2017.07.002.

[4] H. Al-Momani *et al.*, "The efficacy of biosynthesized silver nanoparticles against Pseudomonas aeruginosa isolates from cystic fibrosis patients", *Sci Rep*, vol. 13, no. 1, 2023. doi: 10.1038/s41598-023-35919-6.

[5] B. J. Neves *et al.*, "Automated framework for developing predictive machine learning models for data-driven drug discovery", *J Braz Chem Soc*, vol. 32, no. 1, 2021. https://doi: 10.21577/0103-5053.20200160.

[6] X. Lin, X. Li, and X. Lin, "A review on applications of computational methods in drug screening and design", *Molecules*, vol. 25, 2020. https://doi: 10.3390/molecules25061375.

[7] I. Sushko *et al.*, "Online chemical modeling environment (OCHEM): Web platform for data storage, model development and publishing of chemical information", *J Comput Aided Mol Des*, vol. 25, no. 6, 2011. https://doi: 10.1007/s10822-011-9440-2.

[8] J. Eberhardt, D. Santos-Martins, A. F. Tillack, and S. Forli, "AutoDock Vina 1.2.0: New Docking Methods, Expanded Force Field, and Python Bindings", *J Chem Inf Model*, vol. 61, no. 8, 2021. doi: 10.1021/acs.jcim.1c00203.

[9] K. Sommer, F. Flachsenberg, and M. Rarey, "NAOMInext – Synthetically feasible fragment growing in a structure-based design context", *Eur J Med Chem*, vol. 163, 2019. https://doi: 10.1016/j.ejmech.2018.11.075.

[10] J. J. Irwin *et al.*, "ZINC20 - A Free Ultralarge-Scale Chemical Database for Ligand Discovery", *J Chem Inf Model*, vol. 60, no. 12, 2020. https://doi: 10.1021/acs.jcim.0c00675.

[11] A. Daina, O. Michielin, and V. Zoete, "SwissADME: A free web tool to evaluate pharmacokinetics, drug-likeness and medicinal chemistry friendliness of small molecules", *Sci Rep*, vol. 7, 2017. doi: 10.1038/srep42717.

[12] H. Yang *et al.*, "AdmetSAR 2.0: Web-service for prediction and optimization of chemical ADMET properties", *Bioinformatics*, vol. 35, no. 6, 2019. https://doi: 10.1093/bioinformatics/bty707.

[13] S. Salentin, S. Schreiber, V. J. Haupt, M. F. Adasme, and M. Schroeder, "PLIP: Fully automated protein-ligand interaction profiler", *Nucleic Acids Res*, vol. 43, no. W1, 2015. https://doi: 10.1093/nar/gkv315.

[14] J. Chadha, L. Khullar, P. Gulati, S. Chhibber, and K. Harjai, "Repurposing albendazole as a potent inhibitor of quorum sensing-regulated virulence factors in Pseudomonas aeruginosa: Novel prospects of a classical drug", *Microb Pathog*, vol. 186, 2024. https://doi: 10.1016/j.micpath.2023.106468.

[15] S. Rajamanikandan, J. Jeyakanthan, and P. Srinivasan, "Molecular Docking, Molecular Dynamics Simulations, Computational Screening to Design Quorum Sensing Inhibitors Targeting LuxP of Vibrio harveyi and Its Biological Evaluation", *Appl Biochem Biotechnol*, vol. 181, no. 1, 2017. https://doi: 10.1007/s12010-016-2207-4.

[16] C. M. M. Koh *et al.*, "A data-driven machine learning approach for discovering potent LasR inhibitors", *Bioengineered*, vol. 14, no. 1, 2023. https://doi: 10.1080/21655979.2023.2243416.

[17] A. Vetrivel, J. Ramasamy, S. Natchimuthu, K. Senthil, M. Ramasamy, and R. Murugesan, "Combined machine learning and pharmacophore based virtual screening approaches to screen for antibiofilm inhibitors targeting LasR of Pseudomonas aeruginosa", *J Biomol Struct Dyn*, vol. 41, no. 9, 2023. https://doi: 10.1080/07391102.2022.2064331.

[18] M. Mellini *et al.*, "In silico Selection and Experimental Validation of FDA-Approved Drugs as Anti-quorum Sensing Agents", *Front Microbiol*, vol. 10, 2019. https://doi: 10.3389/fmicb.2019.02355.

[19] G. Daidone *et al.*, "Synthesis, crystallographic studies and biological evaluation of some 2-substituted 3-indazolyl-4(3H)-quinazolinones and 3-indazolyl-4(3H)-benzotriazinones", *Heterocycles*, vol. 43, no. 11, 1996. https://doi: 10.3987/COM-96-7549.

[20] S. A. Patil, R. Patil, and S. A. Patil, "Recent developments in biological activities of indanones", *European journal of medicinal chemistry*, vol. 138, pp.182–198. https://doi.org/10.1016/j.ejmech.2017.06.032